EVALUATION OF FACTUAL PROPERTIES OF FUNCTIONALLY GRADED CARBON NANOTUBE SANDWICH SHELLS USING ROM

1 Ms.C.Sucharitha, Research Scholar, Department of Mechanical Engineering, GITAM University, Hyderabad

E-Mail: naga.sucharitha@mgit.ac.in

Dr.P.Eshwaraiah, Department of Mechanical Engineering, GITAM University, Hyderabad

Abstract

Shell-like structures are commonly used in many mechanical, civil, aeronautical, marine, and architectural engineering applications because they produce optimal dynamic behaviour. Carbon nanotubes (CNT) are used as reinforcing constituents in composite structures such as beam, plate, and shell due to their high strength and stiffness to weight ratio. Because of these CNT characteristics, this research investigated the elastic properties of CNTRSS plate and shell forms. The density, poisons ratio, modulus of elasticity, and remaining elastic properties of functionally graded carbon-nanotube sandwich shells reinforced with PMMA as matrix are investigated in this article. The stacking structures considered are functionally graded with O, X and V form types. Different volume portions such as 12, 17 and 28 were considered as fibre percentage. The CNT's are included in the sandwich shell with different volume fractions and calculated material properties taking reference values from the base journals. Using rule of mixtures theory the formulations were built and solved using a two-step process. The fibres considered in this research are carbon reinforced with CNT.

Keywords: CNT, Sandwich shells, Composite plate, Property, Matrix.

I. Introduction

The structures made of carbon nanotube (CNT) reinforced composites have found considerable application in civil, mechanical, aeronautical and marine engineering due to their exceptional mechanical, heat and electrical properties. CNTs are carbon allotropes found by Iijima [1] with a length scale in the order of nanometres, a higher strength/weight ratio, & a lower density. CNTs are much preferable as a reinforcing alternative for advanced composites due to their better characteristics. Zhu et al. [2] used the finite element approach to investigate the effect of singly walled CNT (SWCNTs) on the bending & vibration analysis of functionally graded carbon nanotube (FG-CNT) reinforced plate. Lei et al. [3] employed the free element Ritz technique to examine the vibration free analysis of a CNT reinforced composite plate with a displacement field based on 1st order shear deformation theory (SDT). Dastjerdi et al [4] used a mesh-free approach to investigate the deflection and strains created in CNT reinforced composite cylinders. Mehrabadi and Aragh [5] investigate the hogging behaviour of a FG-CNT reinforced composite cylindrical shell under the load of mechanical stresses. They calculated using the advanced theory named Eshelby-Mori-Tanaka technique to compute final characteristics of a CNTimparted cylindrical shell. Sb. et.al. [6] applied the Ritz approach to investigate 3D pulsation analysis of a CNT reinforced plate. Natarajan et al. [7] employ HSDT to investigate the static and pulsation free of FGCNTRC sandwich plates. Zhang et al. [8] applied no element Ritz approach with FSDT to investigate the behaviour of a CNT-reinforced plate with elastically fixed edges. Both Selim et al. [9] and Zhang and Selim [10] used Reddy's higher order shear deformable model for mesh-free pulsation analysis of a FG-CNTRC plate. Using FSDT, Mirzaei and Kiani [11] looked into the impact of cut-out on the free vibration of the FG-CNTRC plate. Ansari et al. numerical solution for the vibration analysis of FGCNTRC elliptical plates is presented in their article [12], which also uses the expanded rule of mixture to calculate the effective material properties.

Composite structures with functionally graded carbon nanotube reinforcements

It has been suggested that the mechanical behaviour of structures can be significantly changed by the CNT content and arrangement in a composite [13]. When researchers realised that carbon nanotube content in composite materials was too low for their liking, they began considering ways to improve the macro mechanical quality materials. Functionally graded CNT amalgamated structures were first proposed by a Chinese researcher named Shen [14], who advocated for the use of a gradient in the volume concentration of CNTs within the material. It is because of this that FG-CNTRC research has gained traction in recent decades; the composite now contains a reinforcing agent and a designable property that both parties find satisfactory.

II. Material Modelling

The following schematic diagram represents the FGCNTSS with different stacking sequences such as FG – O, X and V.

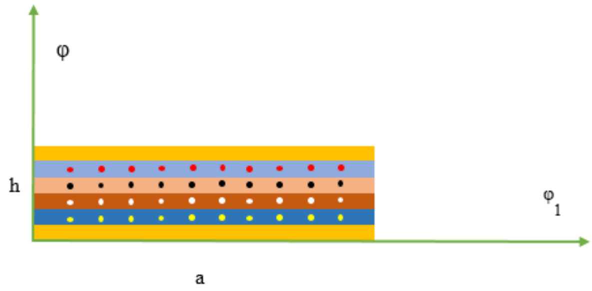

Fig 1. Schematic Representation of FGCNTSS – UD

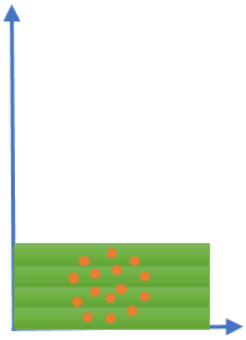

Fig 2. FG – O type

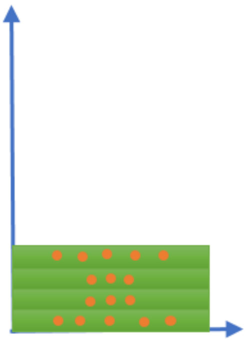

Fig 3. FG – X type

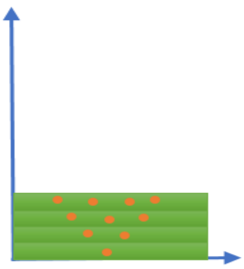

Fig 4. FG – V type

Fig. 1 displays the inclusions of the FGCNT reinforced composite laminates employed in this investigation, which consists of a square with sides a & b and overall width of h. The plate's material coordinates ($\varphi 1$, φ) are determined using its midsection as a reference. In this investigation, we focus on four different distributions of carbon Nanotube configuration within a polymer matrix within a CNT reinforced composite plate along the thickness axis: uniformly distributed (UD), function graded (FG-O), function graded (FG-X), and function graded (FG-V). Using the law of mixture [15, 16], we may make an educated guess as to the ultimate material properties of the FGCNT reinforced composite plate. As shown in the figure 1, the dots indicate the FGM placed at equal distance with different sequence such as X, V, O.

III. Mathematical Modelling

These forms a hybrid model and a new methodology is required to solve such equations. In this, elastic properties are determined using the rule of mixtures for different volume calculation and the respective equations are displayed below. It is believed that the CNTs in the CNTRC plate shown in Fig. 1 have the following three distributions of volume along the thickness direction:

$$V_{CNT}(\varphi)=\left\{V^{*}_{CNT}\right\} \quad \text{(UD) - eq. (1)}$$

$$V_{CNT}(\varphi)=\left\{2\left(1-\frac{2|\varphi|}{h}\right)V^{*}_{CNT}\right\} \quad \text{(FG – O) - eq. (2)}$$

$$V_{CNT}(\varphi)=\left\{2\left(\frac{2|\varphi|}{h}\right)V^{*}_{CNT}\right\} \quad \text{(FG – X) - eq. (3)}$$

$$V_{CNT}(\varphi)=\left\{\left(1+\frac{2|\varphi|}{h}\right)V^{*}_{CNT}\right\} \quad \text{(FG – V) – eq. (4)}$$

$$V^{*}_{CNT}=\frac{w_{CNT}}{w_{CNT}+\left(\delta^{CNT}/\delta^{m}\right)-\left(\delta^{CNT}/\delta^{m}\right)w_{CNT}}$$

Where,

W indicates the weight fraction δ^{CNT} , δ^{m} indicates the polymer matrix density and mass of carbon Nano tubes. By including the CNT competence parameters in the law of mixing, the factual characteristics of the FGCNT reinforced plate may be utilised, and the resulting elastic properties can be written as shown below (with reference to [14]).

$$E_{11}=\eta_1 V_{CNT}E_{11}^{CNT}+V_m E^{m} \quad \text{- eq. (5)}$$

$$\frac{\eta_2}{E_{22}}=\frac{V_{CNT}}{E_{22}^{CNT}}+\frac{V_m}{E^{m}} \quad \text{- eq. (6)}$$

$$\frac{\eta_3}{G_{12}}=\frac{V_{CNT}}{G_{12}^{CNT}}+\frac{V_m}{G^{m}} \quad \text{- eq. (7)}$$

$$v_{12}=V^{*}_{CNT}v_{12}^{CNT}+V_m v^{m} \quad \text{- eq. (8)}$$

$$\rho_{12}=V^{*}_{CNT}\rho_{12}^{CNT}+V_m \rho^{m} \quad \text{- eq. (9)}$$

Where E_{11}^{CNT} , E_{22}^{CNT} G_{12}^{CNT} are the young's modulus and shear modulus of sandwich carbon Nano tubes, E^{m} , G^{m} are young's modulus and shear modulus of polymer matrix. The ŋ1, ŋ 2 and ŋ3 are the efficiency parameters of reliant on material properties. v & ρ are the poisons ratio and mass density of matrix and SWCNT. V_{CNT} ρ_{12}^{CNT} are known as volume portions of the CNT and reinforcement.

Some of the apparent inconsistencies in the theory of first-order shear deformation become more pressing when dealing with reasonably dense shields or bonded structures with a low transverse shear modulus at their core. By eliminating Kirchhoff's third element, the transverse normal in the Mindlin – Reissner theory, commonly known as the FSDT, does not deform, remain perpendicular to the mid-surface. Transverse shear strains are created in this manner. Although the thickness z direction experiences a continual displacement, the inextensibility of the oblique normal persists. Displacement field for FSDT is

$$u_x = (x,y,z) = u_{x0}(x,y) + \phi_x(x,y)z \quad \text{- eq. (11)}$$

$$u_y = (x,y,z) = u_{y0}(x,y) + \phi_y(x,y)z \quad \text{- eq. (12)}$$

$$u_z = (x,y,z) = u_{z0}(x,y) \quad \text{- eq. (13)}$$

Unknowns will include the values of u_{x0}, u_{y0}, u_{z0}, ϕ_x, ϕ_y. The rotation functions ϕ_x, ϕ_y should approach the respective slopes of the transverse deflection $\frac{-\partial u_{z0}}{\partial x}$ $\frac{-\partial u_{x0}}{\partial x}$ at thin areas where the ratio of the plate's in-plane characteristic dimension to its thickness is on the order of 50 or larger. According to FSDT, linear distributions for u_x, u_y, and u_z can be shown in the figure below. Additionally, the physical significance of the ϕ_x, ϕ_y rotations was illustrated.

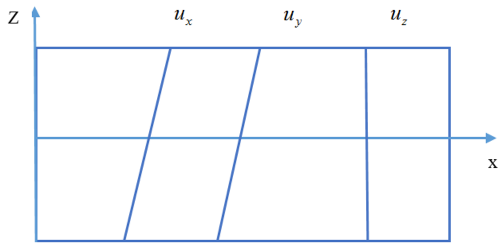

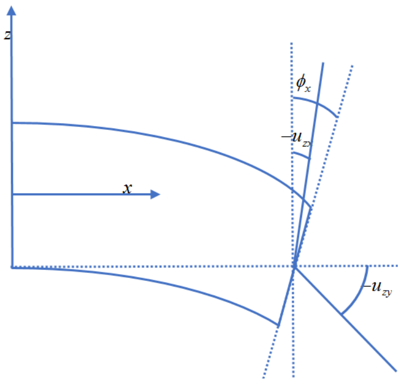

Figure 5. Distribution of displacements in FSDT technique

By imparting the displacement field into the geometrical relations, the strain components can be derived. Only strain ε_{zz} is zero, so the not-null strains are as follows.

$$\varepsilon_{xx} = \frac{\partial u_x}{\partial x} = u_{xo,x} + \phi_{x,x} z$$

$$\varepsilon_{yy} = \frac{\partial u_y}{\partial y} = u_{yo,y} + \phi_{y,y} z$$

$$\gamma_{xy} = \frac{\partial u_x}{\partial y} + \frac{\partial u_y}{\partial x} = u_{xo,x} + u_{yo,y} + \phi_{x,y} z + \phi_{y,x} z$$

The in-plane and shear stress elements are calculated using the constitutive relations.

$$\begin{Bmatrix} \sigma_{xx} \\ \sigma_{yy} \\ \tau_{xy} \end{Bmatrix} = \frac{E}{1-v^2} \begin{bmatrix} 1 & v & 0 \\ v & 1 & 0 \\ 0 & 0 & \frac{1-v}{2} \end{bmatrix} \begin{Bmatrix} \varepsilon_{xx} \\ \varepsilon_{yy} \\ \gamma_{xy} \end{Bmatrix}$$

$$T_{xz} = kG\gamma_{xz}$$

$$T_{yz} = kG\gamma_{yz}$$

There is a shear correction factor denoted by. Similar to the TBT, the shear predicted by the FSDT needs to be modified so that it satisfies the stress-free boundary conditions on the unloaded top and bottom faces of the plate. This shear is projected to be constant along the thickness, but in fact it must be at least parabolic. Numerous ways exist to calculate for the

FSDT in the collected works. Though this article does not directly address the shear correction factor, it does illustrate that higher-order models are often used to avoid its inclusion.

IV. Results & Discussions

All mechanical properties and stress, strain values of the FGCNT at static condition. The material properties are formulated for each structure and represented in the table shown below. As the total height of the functionally graded carbon nanotube sandwich shell is of height h, and the length of the beam is 1m, the slenderness ratio is considered as 6. Therefore l/h = 6 and h is defined as 1/6 from the above formula. The below is the figure for the x – structure sandwich plate with all the referral limits.

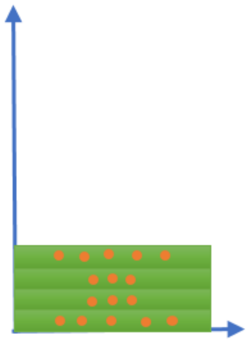

Fig 6. FG – X type

The total length of the plate is 1m, the boundary limits of the plate will be h/2 to –h/2. This indicates the height of the sandwich plate is taken from the mid plane. By considering the different volume fractions of 0.12, 0.17 and 0.28, the material properties of the x structure is displayed in the below.

For volume fraction (V^*_{CNT}) – 0.12

$$V_{CNT} = 2\left(\frac{2(\varphi)}{h}\right).V^*_{CNT}$$

$$V_{CNT} = 2\left(\frac{2(\varphi)}{h}\right).0.12$$

$$V_{CNT} = \frac{0.48\varphi}{h} \text{ - eq. (14)}$$

As we already know that,

$$V_m + V_f = 1$$

$$V_m = 1 - V_f$$

$$V_m = 1 - V_{CNT}$$

$$V_m = 1 - \frac{0.48\varphi}{h} \text{ - eq. (15)}$$

The elastic moduli of the FGCNTRSS is found using the rule of mixtures method from the mechanics of composite materials. Using the same principle, Poisson's ratio and density of the CNTRC beams are written as:

$$\rho = V_{CNT}.\rho^{CNT} + V_m.\rho^m \quad \text{eq. (16)}$$

$$\nu = V_{CNT}.\nu^{CNT} + V_m.\nu^m \quad \text{eq. (17)}$$

When carbon nanotube reinforcement is arranged in the various patterns depicted in Figure 3 for the beam's cross sections.

For x structure:

$$V_{CNT} = 2\left(\frac{2(\varphi)}{h}\right).V^*_{CNT}$$

For O Structure:

$$V_{CNT} = 2\left(1 - 2\frac{\varphi}{h}\right)V^*_{CNT}$$

For V structure:

$$V_{CNT} = \left(1 + \frac{2\varphi}{h}\right)V^*_{CNT}$$

Density

As the density is represented by ρ the equation 16, substitute eq. 14 & 15 in 16 and reformulate which is given as,

$$\rho = \frac{100.8\varphi}{h} + 1190$$

Now to enhance the equation, integrate the above equation using the limits –h/2 to h/2 which is the height of the FGSWS.

$$\int_{-h/2}^{h/2} \rho = \int_{-h/2}^{h/2} \left(\frac{100.8\varphi}{h} + 1190\right)$$

By formulating the above equation, density is defined in terms of h. where h is predefined as 1/6. Now include h in the above equation and reformulate and density is defined as 198.33 Kg/m^3.

$$\rho = 1190h$$

$$\rho = 198.33 Kg/m^3$$

Poisson Ratio

The poison ratio is represented by ν, ν_{CNT} is 0.19 [17], ν_m is 0.3 [17] is taken as reference values to calculate the poison ratio. By substituting equations 1 & 2 in equation 17, it is represented as follows.

$$\nu = 0.3 - \frac{0.0516\varphi}{h}$$

Now the above equation is integrated with limits –h/2 to h/2 and the final equation is represented as follows. Including the h value as 1/6 in the below equation displays the poison ratio.

$$\nu = 0.3h$$

$$\nu = 0.05$$

Calculate E_{11}^{CNT}

The following are the effective material parameters of CNT reinforced sandwich shells at ambient temperature that are used in this paper. The matrix material is poly methyl methacrylate (PMMA), which is known for its: $\nu^p = 0.3$, $\rho^p = 1190 Kg/m^3$,[17] $E^p = 2.5GPa$. For strengthen material, SWCNT having properties $\nu^{CNT} = 0.19$, $\rho^{CNT} = 1400 Kg/m^3$, $E_{11}^{CNT} = 600GPa$, $E_{22}^{CNT} = 10GPa$, $G_{12}^{CNT} = 17.2GPa$ [18].

In this study, the CNT proficiency limits (η_i) allied with the given volume fraction (V_{CNT}^*) is displayed in the below table [15].

Table 1. Efficiency values at different volume fractions [15]

Volume Fraction (V_{CNT}^*)	η_1	η_2	η_3
0.12	1.2833	1.0556	1.0556
0.17	1.3414	1.7101	1.7101
0.28	1.3238	1.7380	1.7380

By substituting the above tabular in the equation 5, E11 is formulated as follows.

$$E_{11} = \frac{368.39\varphi}{h} + 2.5, E_{22} = \frac{26.415h}{10h - 3.6\varphi},$$

$$G_{12} = 1.794 - \frac{1.0556h}{0.2552\varphi}$$

Similarly, place n1, n2 and n3 values in equations 5, 6 and 7 represents E11, E22 and G12. Now integrating the above equation with limits –h/2 to +h/2 gives the final output in terms of h. keeping in mind the value of h as 1/6. The final E11 is displayed as follows.

$$\int_{-h/2}^{h/2} E_{11} = \int_{-h/2}^{h/2} \left(\frac{368.39\varphi}{h} + 2.5 \right)$$

$$\left(E_{11} = \frac{368.39\varphi^2}{2h} + 2.5\varphi \right)_{-h/2}^{h/2}$$

$$E_{11} = 2.5h$$

$$E_{11} = 0.416GPa$$

$$\int_{-h/2}^{h/2} E_{22} = \int_{-h/2}^{h/2} \left(\frac{26.415h}{10h - 3.6\varphi} \right)$$

$$E_{22} = \left(\frac{52.83h\varphi}{20h\varphi - 3.6\varphi^2} \right)_{-h/2}^{h/2}$$

$$E_{22} = 5.459GPa$$

$$\int_{-h/2}^{h/2} G_{12} = \int_{-h/2}^{h/2} \left(1.794 - \frac{1.0556h}{0.2552\varphi} \right)$$

$$G_{12} = \left(1.794 - \frac{4.224h\varphi}{0.2552\varphi^2} \right)_{-h/2}^{h/2}$$

$$G_{12} = 1.794h$$

$$G_{12} = 0.299GPa$$

Similarly the material properties for the o and v structure are found using the above equations 5, 6 and 7 by inserting the tabular data which is finally represented as follows.

Table 2. Material properties of x structure at different volume fractions

Volume Fraction	**Density (Kg/m^3)**	**Poisson ratio**	**E_{11} (GPa)**	**E_{22} (GPa)**	**G_{12} (GPa)**
0.12			0.416	5.49	0.299
0.17	198.33	0.05	0.487	9.05	0.425
0.28			0.635	12.50	0.605

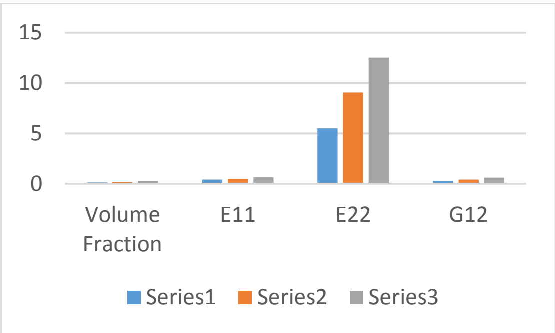

Table 3. Material properties of V structure at different volume fractions

Volume Fraction	**Density (Kg/m^3)**	**Poisson ratio**	**E_{11} (GPa)**	**E_{22} (GPa)**	**G_{12} (GPa)**
0.12			15.765	31.86	4.023
0.17	202.6	0.0478	18.46	45.08	7.23
0.28			23.22	51.25	10.54

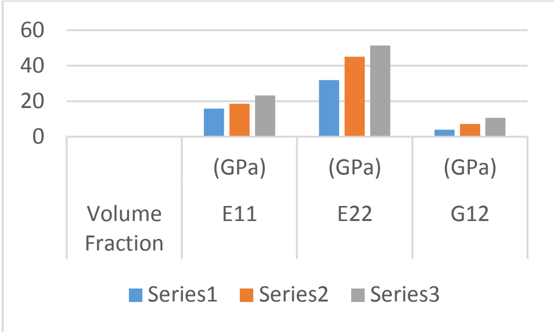

Table 4. Material properties of O structure at different volume fractions

Volume Fraction	**Density (Kg/m^3)**	**Poisson ratio**	**E_{11} (GPa)**	**E_{22} (GPa)**	**G_{12} (GPa)**
0.12			31.115	29.322	99.25
0.17	206.733	0.1368	45.26	35.54	135.62
0.28			58.64	46.28	175.22

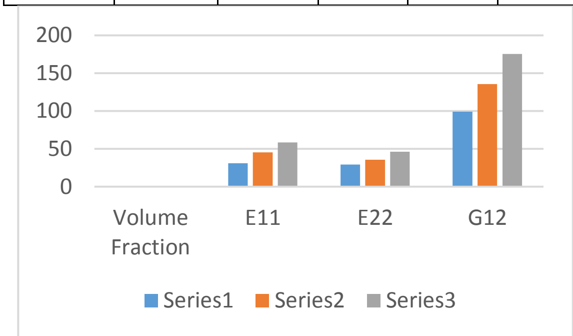

V. Conclusions

Thickness-gradient assumptions and the law of mixing are used to approximate FG-material CNTRC's properties. As the volume fraction and type of structure changes the material properties are gradually changing in an increasing order. The results indicate that elastic properties changes w.r.t the volume fraction. As the type of structure changes E11, E22 and G12 are gradually increasing. Given that FG-CNTRC material is composed of SWCNTs with a random orientation, the effective elastic characteristics are calculated using the rule of mixtures approach. Effective elastic characteristics of FG-CNTRHC material taking into account randomly oriented SWCNTs are obtained using the ROM method in conjunction with the strength of material approach.

It has been observed FG O type of distribution provides higher elastic properties compared to other distribution under consideration. It has been discovered that the physical properties of FGCNTSS are strongly influenced by the volume percentage of CNTs. This holds true regardless of the distribution pattern of the CNTs. FG's Material Effectiveness Material properties of CNTRHC have been established by taking into account the carbon fibre volume fraction follows a power law distribution and the fibre orientation along the thickness direction in such a hybrid FG shell structure. The research shows that the volume proportion of CNTs and carbon fibres affects all of the elastic characteristics of the hybrid composite, and that a smooth variation of transformed elastic properties is obtained, which is desirable for preventing delamination of the laminated composite structure. Further investigations can be done on the analysis such as free vibrations and bending behaviour of composites.

VI. References

[1] S. Iijima, Helical microtube of graphitic carbon, Nature. 354 (1991) 56–58.

[2] P. Zhu, Z.X. Lei, K.M. Liew, Static and free vibration analyses of carbon nanotube-reinforced composite plates using finite element method with first order shear deformation plate theory, Compos. Struct. 94 (2012) 1450–1460.

[3] Z.X. Lei, K.M. Liew, J.L. Yu, Free vibration analysis of functionally graded carbon nanotube-reinforced composite plates using the element-free kp -Ritz method in thermal environment, Compos. Struct. 106 (2013) 128–138.

[4] R. Moradi-dastjerdi, M. Foroutan, A. Pourasghar, R. Sotoudeh-bahreini, Static analysis of functionally graded carbon nanotube reinforced composite cylinders by a mesh-free method, J. Reinf. Plast. Compos. 32 (2013) 593–601.

[5] S.J. Mehrabadi, B.S. Aragh, Thin-Walled Structures Stress analysis of functionally graded open cylindrical shell reinforced by agglomerated carbon nanotubes, Thin Walled Struct. 80 (2014) 130–141.

[6] E.A. Shahrbabaki, A. Alibeigloo, Three-dimensional free vibration of carbon nanotube-reinforced composite plates with various boundary conditions using Ritz method, Compos. Struct. 111 (2014) 362–370.

[7] S. Natarajan, M. Haboussi, G. Manickam, Application of higher-order structural theory to bending and free vibration analysis of sandwich plates with CNT reinforced composite facesheets, Compos. Struct. 113 (2014) 197–207.

[8] L.W. Zhang, W.C. Cui, K.M. Liew, Vibration analysis of functionally graded carbon nanotube reinforced composite thick plates with elastically restrained edges, Int. J. Mech. Sci. 103 (2015) 9–21.

[9] B.A. Selim, L.W. Zhang, K.M. Liew, Vibration analysis of CNT reinforced functionally graded composite plates in a thermal environment based on Reddy ' s higher-order shear deformation theory, Compos. Struct. 156 (2016) 276–290.

[10] L.W. Zhang, B.A. Selim, Vibration analysis of CNT-reinforced thick laminated composite plates based on Reddy 's higher-order shear deformation theory, Compos. Struct. 160 (2017) 689–705.

[11] M. Mirzaei, Y. Kiani, Free vibration of functionally graded carbon-nanotube-reinforced composite plates with cutout, Beilstein J. Nanotechnol. 7 (2016) 511–523.

[12] R. Ansari, J. Torabi, A.H. Shakouri, Vibration analysis of functionally graded carbon nanotube-reinforced composite elliptical plates using a numerical strategy, Aerosp. Sci. Technol. 60 (2017) 152–161.

[13] Lau KT, Lu M, Hui D. Coiled carbon nanotubes: synthesis andtheir potential applications in advanced composite struc-tures. Compos Part B Eng. 2006;37(6):437–48.

[14] Shen H. Nonlinear bending of functionally graded carbonnanotube-reinforced composite plates in thermal environ-ments. Compos Struct. 2009;91(1):9–19.

[15] M.M. Ardestani, L.W. Zhang, K.M. Liew, Isogeometric analysis of the effect of CNT orientation on the static and vibration behaviors of CNT-reinforced skew composite plates, Comput. Methods Appl. Mech. Engrg. 317 (2017) 341–379.

[16] B. Huang, Y. Guo, J. Wang, J. Du, Z. Qian, T. Ma, L. Yi, Bending and free vibration analyses of antisymmetrically laminated carbon nanotube-reinforced functionally graded plates, J. Compos. Mater. 51 (2017) 3111–3125.

[17] Wattanasakulpong, Nuttawit; Ungbhakorn, Variddhi (2013). Analytical solutions for bending, buckling and vibration responses of carbon nanotube-reinforced composite beams resting on elastic foundation. Computational Materials Science, 71(), 201–208. doi:10.1016/j.commatsci.2013.01.028..